Seamless Multimodal Transit from Roads to High-Speed Tunnel Corridors

Adam B. Suppes and Galen J. Suppes

***Abstract*— Ground effect flight is able to seamlessly operate across America's existing roadway, railway, water, and air corridors; but barriers emerge on transfers to and from low-pressure tunnels. The barriers may be overcome using open entrances/exits to/from lower-pressure tunnels and higher-pressure surroundings, which is possible when Bernoulli loops use air's dynamic pressure to sustain pressure gradients in steady-state operation. The resulting seamless transfer from the vast array of road/rail/water/air multimodality to low pressure tunnel transit includes use of perpetual tunnel tailwinds and resulting transit faster than today's best airliners or maglev transit. This includes seamless non-stop transit between any of America's many subway and port stations using existing widespread infrastructure. Computational fluid dynamics (CFD) of digital prototypes confirm both: a) the viability of open-entry low-pressure tunnels and b) operation of ground-effect flight transit (GEFT) at energy efficiencies higher than any alternative at velocities in excess of 60 mph. Extended advantages include: a) inexpensive and quick deployment strategies, b) widespread electrification of markets currently served used diesel and aviation fuel, and c) expedited timelines to a zero-carbon-footprint society.**

***Index Terms*— Bernoulli Loops, Ground Effect, High Speed, L/D Efficiency, Multimodal, Rail.**

I. INTRODUCTION

GROUND effect machines (GEM) include hovercraft as well as vehicle variations that use oncoming air' dynamic pressure to sustain lower-cavity pressures when traveling faster than ~60 mph. Traditionally, GEM have been either inefficient or have interior heights too low for passenger and freight payloads [1, 2]. GEFT, see Figure 1, use an upper-surface trailing-section ducted fan to push air over a trailing taper/ramp to truncate vehicle length while reducing drag and generating aerodynamic lift. Energy efficiency is markedly increased due to reductions in drag and rolling losses. The most efficient operation is over railway tracks due to the low clearance possible when cavity fence (aka, skirt) locations are coupled with tires—tires may replace steel wheels since rolling losses are alleviated with aerodynamic suspension.

Unprecedented high speeds are possible on old rail infrastructure since 2-8 ton GEFT vehicles using aerodynamic lift exhibit less than 1% of the stress on tracks versus 400-ton trains. GEFT tires, rather than steel wheels, offer further advantages of smoother rides, reduced noise, and increased traction. Optimal operation uses GEFT's ducted fan to establish flow behind the vehicle without jetwash and with velocities near surrounding air velocity; the ducted fan propulsion is supplemented with wheel or linear motor propulsion to create these low-noise, low-lost-work modes of operation.

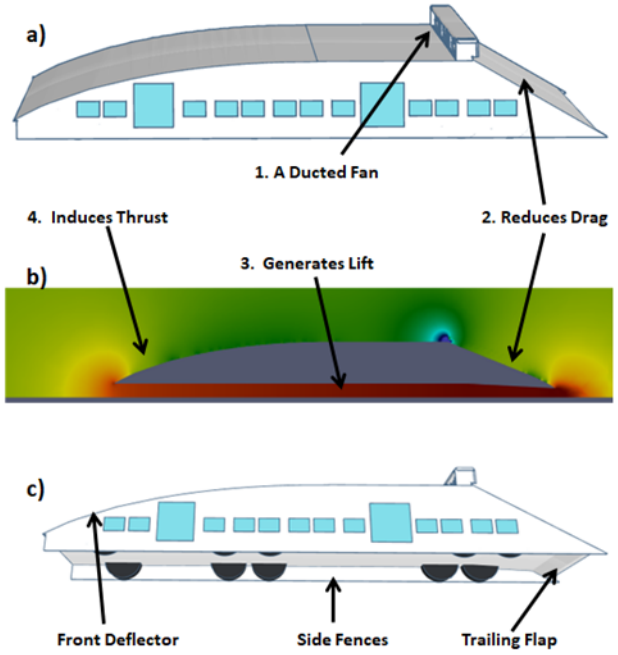

Fig 1. Illustration of ground-effect flight transit vehicle (GEFT) and its enabling pressure profile where red, yellow, and blue are higher, neutral, and lower pressure differences from surroundings.

Subways provide convenient access throughout many cities, and so, multimodal ground-effect vehicles capable of engaging subway tracks could offer a path of transit evolution with exceptionally high connectivity, low transit times and low energy consumption. New scheduling approaches allow non-stop express routing between dozens of stations on a single track, reducing passenger end-to-end transit times to all-time lows with resulting high money-value-of-saved-time using existing infrastructure [3]. Multimodality allows the GEFT to leave tracks, proceeding via slabs and roadways for additional routing and turn-around options. Also, since ground-effect flight transit (GEFT) vehicles do not have undercarriages or wheels, the prospect exists to split single-track tunnels into two over-under tracks, increasing routing options and capacities.

For intercity transit, tunnel corridors, which operate at lower pressures and perpetual tunnel tailwinds, enable speeds faster than airliners. The prospect is for non-stop passenger-oriented end-to-end transit at speeds faster than airliners, including shorter commuter distances. The enabling technologies for this extreme multimodality are: a) multimodality as enabled with rubber tires with low rolling losses due to aerodynamic suspension (see Figure 1), b) advances in scheduling enabling a dominance of non-stop end-to-end transit, and c) Bernoulli Loop technology allowing lower pressure tunnels to operate with open vehicle entrances and exits [3, 4]. This paper provides digital prototype simulations of related tunnel transit

and Bernoulli Loop operation.

II. Background

Ten papers over a 2-year period document the use of computational fluid dynamics to evolve the following strategic advances toward the multimodal transit technology of this paper:

- a fundamental foundation that enables accurate extrapolation as part of design and innovation processes [5, 6],
- ground effect flight vehicles (i.e. GEFT) which allow all-time lows in drag and rolling losses for highway and railway transit. The same aerodynamics that reduce drag also create aerodynamic lift [7-13]. and
- scheduling that allows system-wide, non-stop, high-speed transit on single tracks of common standard railway infrastructure [3].

These advances enable technologies such as trucks, trains, and automobiles that can be fully powered by direct solar energy on sunny days [14]. Two technologies of this paper provide the path to take this technology to the next level:

- Digital prototypes of GEFT operation in tunnels to understand how to sustain efficient ground-effect flight in tunnels, and
- digital prototypes of Bernoulli Loop entrances and exits to allow open entry to lower-pressure tunnels enabling speeds faster than today's airliners (due to perpetual maintainable tunnel tailwinds).

Both are topics of tunnel transit.

A. Tunnel Transit

Tunnel and tube transit typically fall into three categories [15]:

- Wheel-based trains or cars passing through tunnels with entrances open to the surroundings.
- Pneumatic transit where air pressure pushes vehicles or cannisters through tubes.
- Isolated low-pressure tunnels, like hyperloop, claiming advantages of high energy efficiency from a massive reduction in aerodynamic drag.

This paper presents a fourth type of transit through tunnels:

- Ground-effect flight transit (GEFT) through tunnels with any of the following modes of operation:
  - Category A - Transit with essentially zero air flow through the tunnels.
  - Category B - Transit with net air flow in the direction of vehicle travel.
  - Category C - Transit with air flowing in the direction opposite the vehicle travel direction.

Category A has advantages when opposite-direction tracks are not separated by walls and when air flow through platform areas is problematic [16]. Category B is for extended tunnel transit and can be a passively forming and stable air flow at optimal conditions of operation. Category C is undesirable.

The ability to operate at desired air flow Category B is a design degree of freedom where GEFT's ducted fan (see Figure 1) thrust relative to supplementary propulsion determines the mode. Supplementary propulsion may include: a) wheel propulsion, b) linear motor propulsion, and c) pneumatic propulsion.

Figure 2 is a benchmark 3D computational fluid dynamic simulation above open ground. A first key feature of this simulation are the similar near-ambient pressures at one fourth the vehicle chord distance in front and behind the GEFT; that simulation result is consistent with Category A performance and Category B performance with pneumatic propulsion supplement.

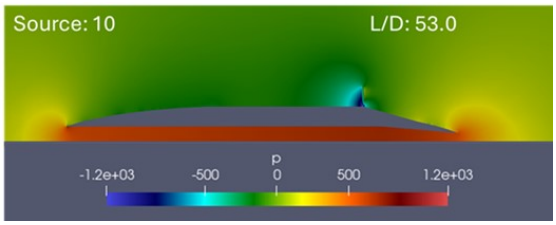

Fig. 2. Example of a high L/D benchmark pressure profile. A cross section of a 3D prototype simulation using fences to block losses of lower compartment lift pressures. Free stream velocity is 40 m/s and the propulsor is in m^4/s^2.

The Figure 2 L/D = 53 is an artifact of lower thickness ratios (fuselage height divided by fuselage chord, e.g. TR = 0.055) and higher aspect ratios (fence ground clearance divided by fuselage height, e.g. AR = 1.0). Combinations of TR and AR consistent with railcar operations are provided by Table 1.

TABLE 1
EXAMPLE DIGITAL PROTOTYPE PERFORMANCES OF GEFT RAILCARS. W IS WIDTH, H IS HEIGHT, CH IS CHORD, AR = W/H, TR=H/CH, CR IS CLEARANCE DIVIDED BY HEIGHT, AND S IS SOURCE POWER IN M4/S2.

AR	TR	Propulsor	CR	L/D	S
0.2	0.11	No	0.01	17.1	N/A
0.2	0.11	Yes	0.01	25.4	2.5
0.3	0.2	Yes	0.01	14.7	10
0.3	0.1	Yes	0.02	34	10

A second key feature of the Figure 2 pressure profile is the pairing of well-formed leading and trailing stagnation points where: a) pressure gradients on frontal and trailing surfaces decrease from higher pressures at lower-surface stagnation points to upper-surface lower pressures and b) a lower-cavity pressure is near air's dynamic pressure throughout the cavity. Effective designs have very low pressure drag on the steeper frontal and rear surfaces, which is possible when the surface integral of higher pressures on the steeper surfaces is similar in magnitude to the surface integral of lower pressures.

A third key feature of the Figure 2 pressure profile is the absence of a trailing jet wash from the propulsor; this feature is observed by the pressure profile rather than explicitly illustrated as from velocity profiles. Jet wash is a trailing high-velocity stream which ultimately is lost work and representative of either inefficient cruising or a necessary loss to achieve high acceleration.

These three key features are mutually consistent with optimal operation, high energy efficiency, and minimal lost work. They are more-easily attained in ground-effect transit above a flat surface since the surface facilitates consistent formation of the trailing-edge stagnation point and assists with streamlining.

B. Bernoulli Loops

Figure 3 illustrates Bernoulli Loops and preliminary performance simulations [17, 18]. The pressure profiles illustrate a reduction in pressure for the tunnel corridor to and from the entrance and exit. The driving force leading to the

mass transfer of air velocity in the tunnel sections; that same air velocity is a favorable tunnel tailwind for vehicles in the tunnel.

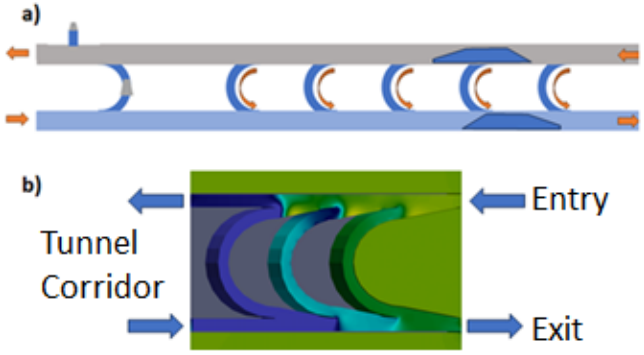

Figure 3. Illustration of Bernoulli Loop tunnel entrance as coupled with a tunnel exit including: a) schematic of the system and b) CFD pressure profiles of performance (blue is lower pressure).

Figure 3a illustrates two blowers. The upper one is not required for operation, however it creates a degree of freedom in operation. The left blower between corridors is not necessary, but can be an efficient means to augment the GEFT's ducted-fan propulsion with pneumatic air flow created by that circulating blower. Air flow in the tunnels must be augmented to compensate for lost work in the Bernoulli Loop scheme; two means to augment the flow are with a blower or with magnetic or traction forces on the vehicles.

The shape and position of the Bernoulli Loops transform flowing air's velocity (i.e., dynamic pressure) into a pressure driving force for transfer of air from the entrance section to the exit section. This pressure-velocity conversion occurs routinely in pipe flow, such as flow through elbows, and can occur with low lost work.

Optimal values of the passively-forming lower pressures and air velocities in tunnels formed by Bernoulli Loops are highly dependent on: a) the length of the tunnel, b) travel speeds of the vehicles, and c) traffic density. Some air is needed to form aerodynamic lift on the GEFT. Preliminary estimates place optimal pressures as being in the range from 0.2 to 0.8 atm. As compared to lower pressures, these pressures have greater benefits from tunnel tailwinds, have air momentum to supplement vehicle momentum to be robust against any sudden leaks in tunnel pressure, and provide an air source to replenish air in passenger compartments.

The goal of this paper is to identify L/D efficiencies for GEFT vehicles in tunnels and to identify if that efficiency is sufficient to realize opportunities for advantages in reduced energy consumption, reduced transit times, and reduced annualized infrastructure costs. A subsequent discussion will bring aspects of Bernoulli Loops into perspective.

. *Rapid Realization of Electric Railcar Deployment*

The approaches of this paper would allow the rapid deployment of electric vehicles without electrification of railway infrastructure at much higher speeds than would otherwise be possible on existing rail infrastructure. The strategy emphasizes major reductions in energy needs which reduces battery weight and costs, and in some instances, enables solar-powered vehicles to make further reductions in battery weights and costs.

Transit in lower pressure tubes is not advocated as preferred, but rather, as a results-driven optimization option that depends on otherwise existent or justified tunnel infrastructure and the evolution toward high-traffic-density high-speed transit corridors. New above-ground transit tubes may have tracks and solar-power surfaces above the upper surfaces of the tubes.

III. Methods

OpenFoam and SimFlow CFD software were used to simulate digital prototypes prepared as STL files. Two-dimensional (2D) simulations were used to identify trends in performance while Three-dimensional (3D) simulations were performed on the final prototypes. Unless otherwise reported, the scale chord of the STLs were 1 m, the fluid was air at 1 atm pressure, and the free stream velocity was 40 m/s.

The ground was simulated as a lower boundary condition "moving wall" with a velocity equal to the free stream air. Tunnel simulation was simulated in 2D using walls as upper and lower boundaries. Propulsors were simulated as cubical geometries that generated horizontal velocities based on the power setting.

Figure 4 provides example CFD meshes which is the initial step in CFD simulation. The meshes illustrate the ground, tunnel's upper surface, and propulsors.

Figure 4 also illustrates the STL, with dimensions, used to generate the 2D mesh. Figure 4 illustrates an example Airfoil. An airfoil, designated "Airfoil B", was used in 2D simulation of ground-effect and tunnel-effect transit. The scale as 1 m in length and 0.1055 m in height includes a 0.01 m cavity height. The propulsor was 0.05 m X 0.005 m for ground-effect and 0.05 m X 0.001 m for tunnel effect. Clearances were 0.006 m from surfaces. Figure 4 provides the meshes for the 2D simulations which show the upper and lower walls of the simulation.

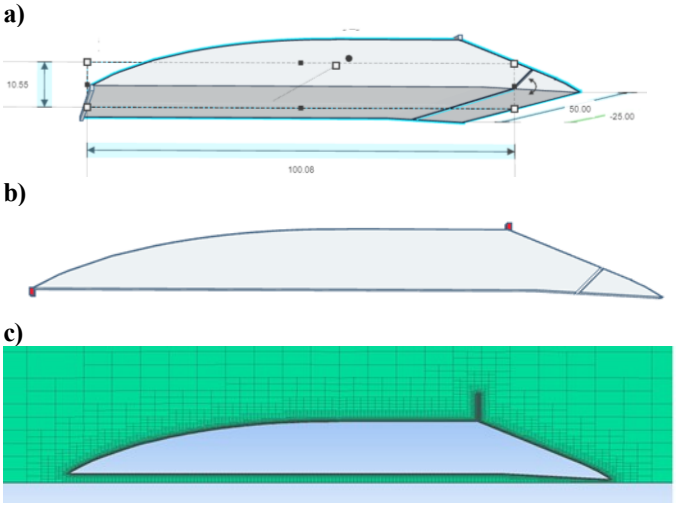

Figure 4. Illustration of: a) computer-aided design (CAD) STL file (standard template library) of lifting body with upper and lower propulsors and a trailing section bypass from the cavity (height = 0.01 m) to the upper surface of the trailing taper, b) a 2D airfoil of the STL, and c) mesh of the 2D airfoil over a bottom ground boundary.

Results from CFD experiment simulations include: lift coefficients (C_l), drag coefficients (C_d), L/D (equal to C_l/C_d), pressure profile images, and velocity profile images. C_l and C_d are calculated from the planform area. Flow around wheels on the

vehicle is not considered under the assumption that air flow can be streamlined between fences and wheels.

All pressure profiles of this paper use a pressure color plat with equal positive and negative magnitudes. This allows conclusions to be drawn from pressure profiles without attention to the magnitude. Vivid red is always higher pressure (relative to free stream pressure), vivid blue is lower pressure, and lime green is free stream pressure. The pressure is reported as P/ρ in units of m2/s2.

2D CFD studies are referred to as "airfoil studies". Airfoil have reduced computational times and are easier to interpret with the assumption of an infinite width wing or lifting body.

In "ground effect" studies fences (aka skirts) on lower cavities block lateral dissipation of pressure, and 2D CFD studies approach the more-accurate 3D prototype studies on lift forces of the lower cavity [9]. In "tunnel effect" studies upper and lower fences are able to black lateral dissipation of lift forces on upper and lower surfaces yielding approachable performance absent details of optimal fence clearances.

For transit in tunnels, the CFD software may generate results that include pushing of air through the tunnel, which is characterized by different pressures at the ends of the tunnel in the CFD mesh. The solution process used in this paper is to converge on vehicle propulsor settings until the pressures distant from the vehicle are equal in the leading and trailing directions such as illustrated by Figure 5.

Figure 5 illustrates a color scale for pressures. The color scale may vary between images; however, the positive and negative magnitudes for the pressure scales are kept equal and opposite. This translates to a lime-green color of zero pressure (P (m2/s2) = pressure divided by air's density, air is at 1 atm).

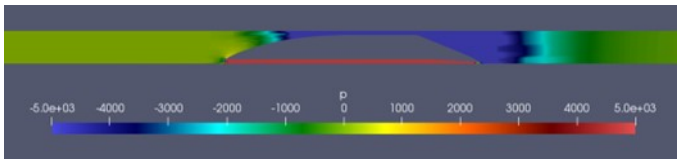

Figure 5. Illustration of relaxing of pressure aft the vessel with an expanded scale for the transit at a propulsor setting of 5.0 m^4/s^2.

Fig. 4b illustrates the STL model with a lower front source ("Lower Propulsor") and an upper trailing-section source ("Upper Propulsor). Two types of rear spoilers were simulated; both are presented in the pressure profiles. An upper rear spoiler is approximately even with the upper surface with about a 0.025 chord gap between the spoiler and the vehicle. A lower rear spoiler was simulated as a flap set back about 0.025 chord lengths from the normal flap position (i.e., see Fig. 4b) in a position to intercept flows from both the lower surface and the trailing taper.

Bypass flows are as illustrated by pressure profiles of the results. A diffuser bypass has a cross-sectional area that increases as flow approaches the bypass exit.

The goal of this paper is to identify approachable performance for variations of GEFT propulsor, spoiler, and diffuser configurations in tunnels. Due to the narrow range of trends, the conclusions are able to exceed the limited range of parameters evaluated in the studies.

V. Results

Tunnel effect simulations of airfoils (2D simulations) are summarized in Table 2 and Figures 6 through 8. Preliminary studies identified that the pressures in the lower cavity of a GEFT of 3D simulations approach 2D simulation results at low clearances (i.e., ratios of clearance to vehicle thickness of <0.005) [9, 10]. In tunnels and with use of fences on the upper surface, the L/D of 3D prototypes will approach the Table 2 results with low fence clearances.

An inspection of the Table 2 reveals the L/D are consistently less than 30. The sequence reported was in the chronology of the experiments and included adapting the design from previous results. For all but the final result, values of L/D in excess of 20 correlated primarily with either the upper or lower clearance being greater than 0.01 m. Lower L/D for these tunnel simulations can be attributed to losses from pushing air around the airfoil to avoid pushing air through the tunnel.

TABLE 2.
SUMMARY OF PROPULSOR SETTINGS AND CLEARANCES OF 2D AIRFOIL SIMULATIONS. THE LOWER CLEARANCE IS THE LOWER WALL LOCATION. THE UPPER CLEARANCE IS THE UPPER WALL LOCATION MINUS 0.115 M (VEHICLE HEIGHT PLUS 0.01 M FOR PROPULSOR HEIGHT.

	Airfoil Descriptor	L/D	Propulsor (m^4/s^2)	Wall Locations (m) Lower, Upper*
a.	Trailing Spoiler	28.0	S=1	-0.004, .215
b.	Trailing Spoiler	23.6	S=2	-0.004, 0.165
c.	Trailing Spoiler	20.0	S=2.5	-0.004, 0.165
d.	Two Spoilers	12.6	S=3	-0.004, 0.165
e.	Two spoilers, Version B	20.4	S=2	-0.004, 0.165
f.	Two spoilers, Version C	22.9	S=2	-0.004, 0.165
g.	Upper & Lower Propulsor	25.5	S=1, S=0	-1.0, 1.115
h.	Upper & Lower Propulsor	28.0	S=1, S=3	-.010, 0.315
i.	Simple Bypass	23.0	S=1.7, S=2.5	-0.004, 0.125
j.	Slanted Bypass	16.0	S=2, S=3	-0.010, 0.125
k.	Diffuser Bypass	20.2	S=0, S=1	-0.004, 0.165
l.	Diffuser Bypass + Spoiler	14.5	S=0, S=2.5	-0.004, 0.165
m.	Spoiler 2	12.0	S=2, S=2	-0.010, 0.125
n.	Cavity Bypass	12.6	S=2, S=3.5	-0.010, 0.125
o.	Cavity Bypass 2	7.0	S=1.5, S=4	-0.010, 0.125
p	Cavity Bypass 3	28.3	S=1, S=3	-0.01, 0.125

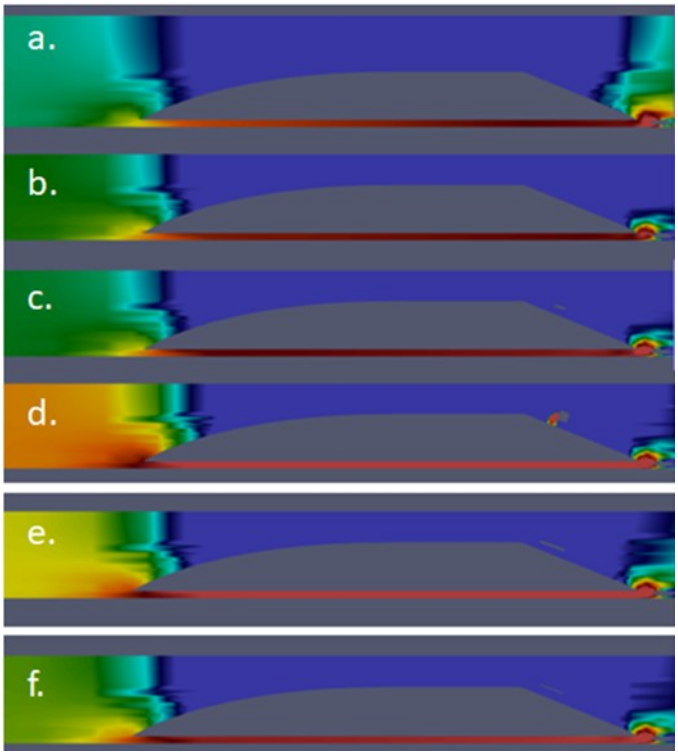

Figure 6. Pressure profiles of converged pressure profiles in tunnels with different upper clearances and different versions of spoilers.

Figure 6 illustrates a persistent lower pressure region above the trailing flap. When good pressure gradients form at the leading section (i.e., pressure gradient with predominance of lower pressures), the predominance of lower pressures on the trailing taper results in increased form drag and decreased L/D.

Various spoiler designs were used to increase L/D. One spoiler option was to extend-rearward the flap section below the vehicle's lower surface to create a gap. That flap/spoiler forms a trailing stagnation pressure point and that pressure expands upward along the trailing taper. The spoilers were effective, improving L/D by about 10%.

Various geometries for a second spoiler were placed above the trailing taper, near the airfoil's upper surface. The spoilers increased pressure above the trailing taper, but the spoilers formed their own trailing-section form drags. Normally that trailing section form drag would not be significant; however, in respect to L/D exceeding 30, the drag becomes relevant.

Figure 7 illustrates various options to use a duct bypass, with a propulsor, through the airfoil to force air dynamics and pressure profiles similar to those of Figure 1. All of these Figure 7 studies were without propulsors at the leading section of the lower cavity. Only the ducts with a diffuser discharge produced good pressure profiles in the lifting body's lower cavity.

In view of these design degrees of freedom, L/D exceeding 30 should be readily attainable.

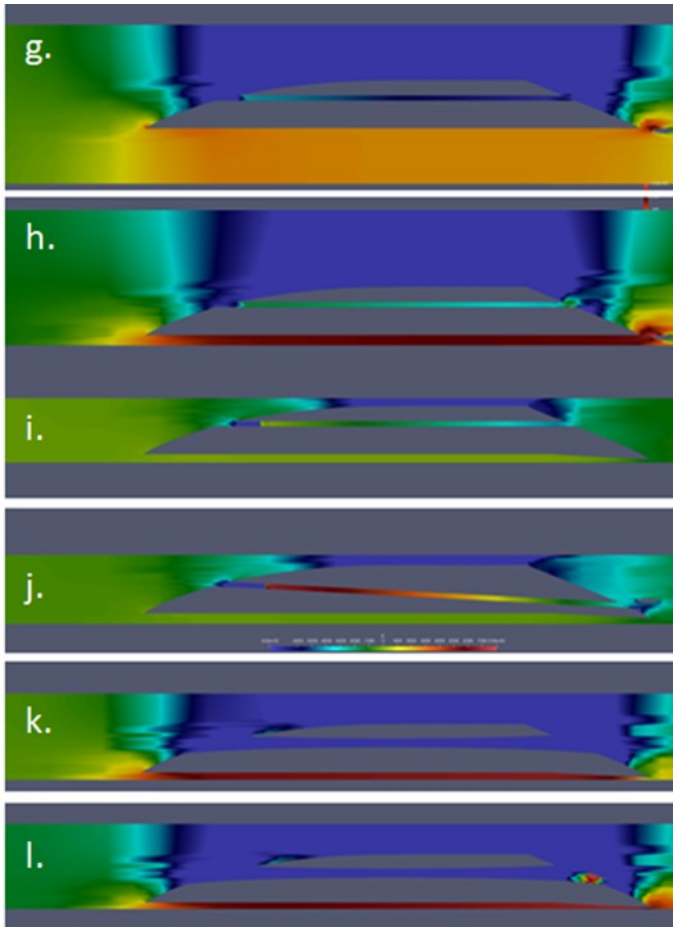

Figure 7. Pressure profiles of converged pressure profiles in tunnel with different clearances and front-to-back duct bypass with bypass propulsors.

Table 2 results m-p summarize use of spoilers and bypasses through the trailing taper from the lower cavity with results similar to a bypass through the vehicle. Conclusions from runs p-m are consistent with an overall conclusion that values of L/D in excess of 20 correlate primarily with either the upper or lower clearance being greater than 0.01 m. However, more information is needed to assess the reason L/D appears to peak around 30 for these 2D simulations.

Table 3 summarizes conditions for simulations q, r, and s for comparison to run p of Table 2. Table 4 summarizes key performance results. Pressure profiles are summarized by Figure 8. Velocity profiles are summarized by Figure 9.

TABLE 3.
SIMULATION CONDITIONS FOR SIMULATION P-S.

		Description
Airfoil		L = 1m, H = 0.1055m (0.0951 without flap).
Sources		L = 0.005 m, H = 0.01 m.
Coordinates		Lowest forward point of airfoil is at x=-0, y=0. (upper walls, lower walls)
Mesh Positions	P:	0.125 m, -0.01 m
	Q:	0.122 m, -0.006 m
	R:	-0.006 m
	S:	-0.006 m

Exceptional performance for GEFT in ground effect is possible because the ground blocks downward dissipation of pressure. A tunnel's upper surface blocks upward dissipation of pressure with the result of higher lift coefficients. However, drag increases disproportionately to lift under the simulation conditions leading to lower L/D efficiency in tunnels.

TABLE 4.
SUMMARY OF SIMULATIONS P-S. $C_{D,V}$ IS THE PERCENT OF TOTAL DRAG WHICH IS VISCOUS DRAG.

	S(m^4/s^2)	L/D	Cl	Cd	Cd,v
P	1, 3	28.3	2.19	0.0776	12%
Q	6.1	36.3	2.48	0.0685	12%
R	0	46.7	1.23	0.0263	16%
S	5	83.0	1.57	0.0190	35%

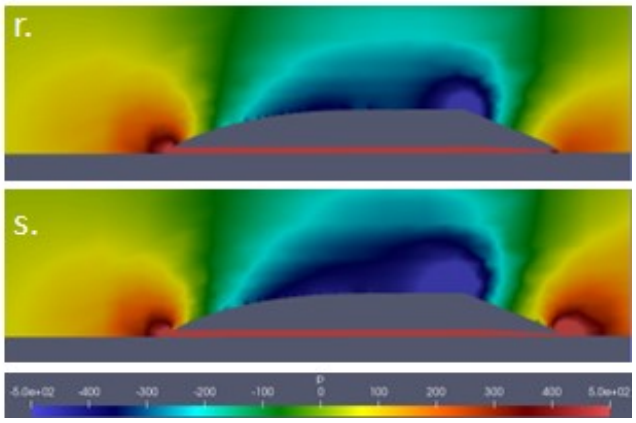

Figure 8. Pressure profiles of digital prototype in ground effect outside tunnel. Pressure is in m^2/s^2.

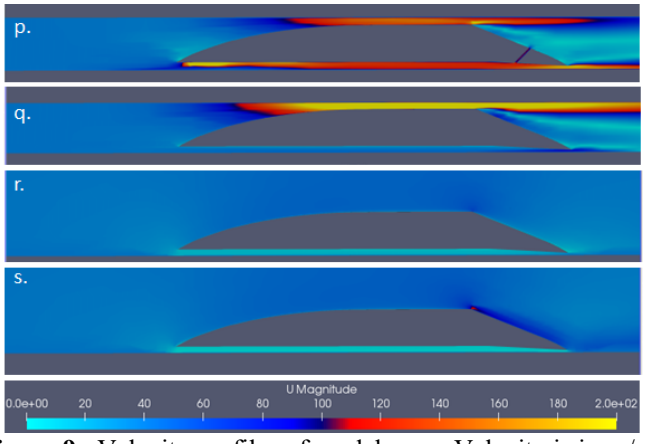

Figure 9. Velocity profiles of models p-s. Velocity is in m/s. Velocity is relative to the vehicle.

The velocity profiles Figure 9 reveal the source of disproportionately high drag in the tunnel as due to the stagnation of air along most of the rear tapered surface; the velocity approaches the velocity of the vehicle with a low pressure acting on the trailing taper.

V. DISCUSSION

Simulation results were limited to 2D simulations which are useful in GEFT ground effect since lower surface lift forces can approach the ideal 2D conditions with lower-cavity fences to block much of the lateral dissipation of the cavity pressures. Similarly, for tunnels, the upper surface pressure profile of actual performance can approach 2D performance.

In 3D simulation, the fence design, fence clearance, flap clearance relative to fence clearance, and aspect ratio impact results. The 2D results isolate more fundamentals and are able to provide important insight.

While "tunnel effect" (i.e., blocking of upward and downward dissipation) was effective in increasing lift coefficients, L/D did not increase relative to "ground effect" alone. L/D failed to increase due to the lost work of jet wash (i.e., ducted fan wash) behind the vehicle where the large velocity gradients trailing the vehicle are lost work. That lost work manifests as increased drag. Simulations r and s did not have similar lost work since boundary layer separation did not occur, and with assistance from the ground, there was a substantial absence of air flow behind the GEFT. In essence, a pressure field around the vehicle with had minimal disturbance to the air due to the passage of the vehicle.

An artifact of achieving high efficiency in GEFT is when the fraction of viscous drag increases (see Table 4), potentially to values in excess of 50%. Both value of drag and L/D can be misleading when ducted fans produce thrust that impacts the pressure field, as is the case for all simulations of this study. Just like boundary layer separation can appear with a minor increase in surface pitch, a minor amount of strategic air flow from a ducted fan can reverse boundary layer separation. For well-designed vehicles, thrust of a ducted fan lost to changing the pressure profile will lead to substantial reductions in drag—the ducted fan propulsion is leveraged by high impacts to pressure profiles from small amounts of thrust.

The L/D values for the tunnel simulations (p, q) are closer to achievable performances than are the ground effect simulations (r, s). Furthermore, there are many degrees of freedom to impact the aerodynamics behind the vehicle to substantially eliminate the lost work from velocity gradients. The most effective degrees of freedom will likely include effective use of fans on the sides of the vehicle since higher air flow is required around the vehicle fill the increased air cross section in the tunnel absent the vehicle cross section.

Additional degrees of freedom include providing overall tailwinds within tunnels to allow higher speeds with similar efficiencies. This includes the potential of trans-sonic speeds without worrying about the dynamics of superseding the sound barrier: a 100 mph tailwind in a tunnel allows from 350 mph travel with the dynamics of 250 mph equivalents outside the tunnel.

Simulation q achieved an L/D of 36 with higher values possible based on the amount of lost work in the jet wash behind the vehicle.

In practice, the lift coefficients of a well-designed ground-effect GEFT system will approach 1.2. For tunnel systems, lift coefficients near 2.0 are possible. An artifact leading to higher lift coefficients is the manner in which the ducted fan creates

higher velocities which can manifest as higher dynamic pressures when those velocities impact the ground behind the cavity's flap (i.e., trailing edge stagnation point). The higher pressures expand forward through the cavity in effective designs.

Ducted Fan Propulsors On GEM – Ducted fans are the preferred propulsors for GEM due to compatibility with electric power and high air throughput. Normally, the primary purpose of a ducted fan is to generate thrust; however, in ground-effect and "tunnel effect" ducted fans have an increasingly important impact on the pressure field over the vehicle's entire surface [19-21].

Table 5 puts this energy efficiency in perspective to other forms of transit where GEFT Subway uses 80% less energy than helicopters and about 40% less than the U.S. average for light rail. Energy costs would be 4 cents/mile and could be provided by 100% renewable electrical power with very low carbon footprints.

TABLE 5.
COMPARISON OF ENERGY EFFICIENCIES [22-25].

Contemporary Vehicles	L/D	Estimated (Btu/passenger-mile)
Multicopters	5	6459
Helicopter	6	5383
Cessna 172	11	2936
Short-Haul Flight		3472
Car		2569
Airliner	15	2153
U.S. Commuter Rail		1583
Bus		1389
Ferry		264
GEFT railway	52	621
GEFT ratilway+ Propulsor	>60	<550
Target GEFT Subway	30	1100

If GEFT subway service were 90 mph non-stop, the time for a 10-mile commute would be 6 minutes versus a typical subway which would be about 21 minutes. The value of 15 minutes at $20/hour is $5 versus GEFT energy costs of $0.40. Table 6 compares numbers for a 10-mile roundtrip under similar assumptions.

TABLE 6
COST METRICS RELATED TO 20-MILE ROUNDTRIP CITY COMMUTE.

Costs for 10-mile Roundtrip Commute	Cost
GEFT Subway Energy, nonstop 90 mph, L/D=30	$0.80
GEFT Subway Energy, nonstop 90 mph, L/D=20	$1.20
GEFT Railway Energy, nonstop 90 mph, L/D=60	$0.40
21-minute subway ride time premium over GEFT Subway	$10
Parking Car Downtown	$10-$20
Fuel cost at $4/gallon, 40 mpg	$2
Car at Government Reimbursement of $0.65/mile	$13
Fuel tax of $0.57/gallon assumed to be 50% of highway cost	$2.08
Air Taxi Commute (helicopter or multicopter) Energy	$4-$6

Within the basis of Table 6, including any reasonable variations, the metrics definitively identify that the true value of high-speed non-stop commute at 90 mph resides in saved time and saved infrastructure, both from utilizing existing infrastructure with multimodal vehicles and mitigating the necessity of developing more single passenger infrastructure (i.e., parking lots and highways). Also, when using electric power, the environmental costs of the GEFT transit energy are small compared to the time value of money and infrastructure depreciation.

The metrics do not include first-mile and last-mile costs; however, the assumption is that route planning would make GEFT mass transit first/last mile costs less than other mass transit. An additional assumption is that solutions like autonomous taxi service will emerge as part of route planning for GEFT mass transit.

GEFT features that would enable a 90-mph non-stop commute using existing infrastructure include:

- Non-stop high-speed transfer between railway, subway, highway, waterway, and greenway corridors.
- Real-time routing based on traffic and preliminary route planning for mass-transit ride share.

A. Air Taxi Comparison

Air taxis have about a 5X increase in energy costs versus GEFT. Air taxis also have major FAA (Federal Aviation Administration) barriers for widespread use over cities and approach restricted air space at many locations. Similar barriers would be reduced or non-existent for GEFT vehicles traveling within a few feet of the ground/water of railway, subway, highway, waterway, and greenway corridors. Here, greenway refers to paths over ditches or select landscape without major obstacle, typically less than a mile, for transfer between transit corridors. It is where the greenways are lacking in city infrastructure that subways provide an effective access alternative.

B. Bernoulli Loop Entrances/Exits

Bernoulli loops are less useful for typical city subway systems since capacity passenger platforms are more-optimally operated at atmospheric pressure. When tunnel sections exceed about 20 miles, benefits of perpetual tunnel tailwinds and lower viscous drag can be realized.

The primary utility of Bernoulli Loops is as an incremental improvement to inter-city high-speed rail transit after the ridership has been established and the return on investment has a high certainty. Travel velocities up to 300 mph are sufficient for transit regions stretching about 1000 miles and can be achieved in atmospheric pressure over mostly already-in-place infrastructure. In the US, three regions likely to rapidly develop regional 300 mph service include an Eastern Region (the greater metropolitan Northeast), a Central Region, and a Western Region (Californian coastal cities). Lower-pressure high-tailwind tunnels would eventually be justified to connect these three regions.

Passenger-oriented end-to-end service can achieve rarely considered higher levels of performance in these networks, such as convenient dining, sleeper cars, and entertainment options for transit over five hours.

Bernoulli loops work best with a continuous and steady flow of vehicles. However, as long as vehicles are present in the entrance before the first loop and after the last loop, the vehicle would contain and utilize pressure differences in those tunnel

sections for acceleration and deceleration. A distance of a few miles prior to the first loop would allow gates to be used to close off those sections with sufficient time for the gate to open and close as soon as a vehicle enters the tunnel.

An advantage beyond speed and efficiency of low-pressure tunnels is the ability to use pneumatic air flow to augment the vehicle ducted fans. A circulating flow, as illustrated by Figure 3 is an effective arrangement for these systems.

For years, low pressure transit has been considered a fringe technology of science fiction. During the past decade hundreds of millions of dollars have been spent attempting to go directly to very low pressures in tunnels with emphasis on supersonic capabilities. The approaches and simulations of this work identify that low-pressure tunnel transit can be incrementally advanced starting with existing tunnel infrastructure and with the ability to identify up front the increased profitability and value of extreme tunnel transit with a ready option to achieve trans-sonic travel speeds without the complications of trans-sonic dynamics.

D. Evolutionary Pathways

Due to the diversity of corridors and the design options, the multimodal GEFT systems of this paper have many paths of evolution. Especially high impact design options on that evolution are:

- Transit through tunnels at low clearance profiles that allow doubling the amount of transit corridors in existing subway and tunnel systems.
- Low-cost overpass routing and intersections in cities where stoplights and stop signs are eliminated.
- Extensions to longer-distance tunnels that use Bernoulli Loops and tail winds to enable velocities greater than used with commercial airliners [26].

V. Conclusion

To attain L/D efficiencies greater than 20, tunnel-GEFT configurations must utilize additional degrees of design freedom than needed with GEFT over open railway tracks. Implicit degrees of freedom for tunnel transit are: a) upper clearance, b) upper fence dimensions, c) lower fence clearance, d) base airfoil shape such as Airfoil B, and ducted fans designed to impact pressure profiles. Design degrees of freedom from ducted fans include duct bypasses and bypasses around vehicle sides. The simulation of fans on the sides of vehicles is beyond the scope of 2D studies.

From a practical perspective, major benefits of GEFT tunnel transit are achieved at L/D greater than 30 with vertical tunnel spans of 3.3 m. Those major benefits include reduced transit time and reduced infrastructure costs due to including subways as part of a multimodal corridor network and enabling non-stop transit in subway tunnels by doubling the number of lanes.

Parallel work on scheduling shows that significant capacity and passenger-oriented nonstop end-to-end transit is possible with single lanes and that L/D efficiencies of 20 are sufficient to enable major advances in multimodal transit with a path of significant upside potential including open access to low-pressure tunnel transit. While the digital prototypes of this paper were only able to achieve L/D near 30 when flying with low upper and lower clearances, higher efficiencies should be possible with ducted fans on vehicle sides.

The exceptional drag reductions of the tunnel transit of this work are augmented by the ability to substantially eliminate rolling losses by replacing the vast majority of wheel suspension with aerodynamic suspension. The advances can accelerate the rate at which benefits can be achieved from electric-powered trains by using fewer batteries and direct solar power.

The results and capabilities summarized in this paper apply to tunnel transit ranging from modification of the operation of subway commuter systems to the prospect of intercity tunnel transit corridors where perpetual engineered tailwinds enable trains to travel faster that today's fastest airliners.

References and Footnotes

References

[1] Blum, A., "Ground Effect Vehicle," 1987,
[2] Anonymous "Ground effect machine," Vol. 7953/71, No. GB1347352, 1974, https://patents.google.com/patent/GB1347352A/en?oq=London+1347352
[3] Suppes, A., and Suppes, G., "GEFT Scheduling to Maximize Value of Current Infrastructure and Upside Potential," *Cambridge Open Engage [Pre-Print],* 2025, https://doi.org/10.33774/coe-2025-x07tg
[4] Kenyon, K.E., "Bernoulli Loops in Smoke Rings," *Natural Science,* Vol. 11, No. 10, 2019, pp. 285. 10.4236/ns.2019.1110030
[5] Suppes, A., Suppes, G., Lubguban, A.A., and Al-Moameri, H.H., "Kinetic theory of gases: explanation of aerodynamic lift," *Aviation (in Review),* 2024,
[6] Suppes, A., Suppes, G., Lubguban, A., and Al-Maomeri, H., "An Airfoil Science Including Causality," *Cambridge Engage,* 2024, 10.33774/coe-2024-w4qtp
[7] Suppes, G., and Suppes, A., "Ground Effect Flight Transit (GEFT) in Subways," Vol. 1, 2024, https://doi.org/10.33774/coe-2024-6w0lw
[8] Suppes, A., and Suppes, G., "Ground Effect Flight Transit (GEFT) – Towards Trans-Modal Sustainability," Vol. 1, 2024, https://doi.org/10.33774/coe-2024-prxvr
[9] Suppes, G., and Suppes, A., "Ground Effect Flight Transit (GEFT) – Approaches to Design," Cambridge University Press, Cambridge Open Engage, 2024. https://www.cambridge.org/engage/coe/article-details/66b2340b01103d79c5e7ab2310.33774/coe-2024-2c87q
[10] Suppes, A., and Suppes, G., "New Benchmarks in Ground-Effect Flight Energy Efficiency," July 102024https://www.researchsquare.com/article/rs-4707178/v1https://doi.org/10.21203/rs.3.rs-4707178/v1 [cited Jul 29 2024].
[11] Suppes, G., and Suppes, A., "Critical Data and Thinking in Ground Effect Vehicle Design," Cambridge University Press, Cambridge Open Engage, 2024. https://www.cambridge.org/engage/https://doi.org/10.33774/coe-2024-76mzx
[12] Suppes, A.B., and Suppes, G., "Thin Cambered Lifting Bodies in Ground Effect Flight," *Engrxix Engineering Archive Pre-Print,* No. 1, 2024, https://doi.org/10.31224/4136
[13] Suppes, A., Suppes, G., and Al-Moameri, H., "Overcoming Boundary-Layer Separation with Distributed

Propulsion," *Sustainable Engineering and Technological Sciences,* Vol. 1, No. 01, 2025, pp. 71–89. 10.70516/7a9e2y30
[14] Afifi-Sabet, K., "New solar-powered EV can drive 40 miles daily using the power of the sun — and it's 50% more efficient than a Tesla," [online database]1737119400https://www.msn.com/en-gb/cars/news/new-solar-powered-ev-can-drive-40-miles-daily-using-the-power-of-the-sun-and-it-s-50-more-efficient-than-a-tesla/ar-AA1xnXjw?cvid=763871DF7B904A97A20F19EDC70003B5&ocid=hpmsn [cited Jan 30 2025].
[15] Shibani, W.M., Zulkafli, M.F., and Basuno, B., "Methods of Transport Technologies: A Review On Using Tube/Tunnel Systems," *IOP Conference Series: Materials Science and Engineering,* Vol. 160, No. 1, 2016, pp. 012042. 10.1088/1757-899X/160/1/012042
[16] Zhou, S., "Dynamics of Rail Transit Tunnel Systems," Academic Press, 2019,
[17] Suppes, A., and Suppes, G., "Ground Effect Machine System," Vol. PCT/US24/62323, 2024,
[18] Suppes, A., and Suppes, G., "Ground Effect Aircraft," Vol. PCT/US24/35242, No. PCT/US24/35242, 2024,
[19] Lachapelle, U., and Boisjoly, G., "Breaking down public transit travel time for more accurate transport equity policies: A trip component approach," *Transportation Research Part A: Policy and Practice,* Vol. 175, 2023, pp. 103756. 10.1016/j.tra.2023.103756
[20] Guerra, E., and Cervero, R., "Cost of a Ride: The Effects of Densities on Fixed-Guideway Transit Ridership and Costs," *Journal of the American Planning Association,* Vol. 77, No. 3, 2011, pp. 267–290. 10.1080/01944363.2011.589767
[21] Membah, J., and Asa, E., "Estimating cost for transportation tunnel projects: a systematic literature review," *International Journal of Construction Management,* Vol. 15, No. 3, 2015, pp. 196–218. 10.1080/15623599.2015.1067345
[22] Davis, S.C., Boundy, R.G., "Transportation Energy Data Book," Oak Ridge National Laboratory, 2022,
[23] Fleck, A., "Chart: Which mode of transport is the most polluting?" *Statista,* 2024, https://www.statista.com/chart/32350/greenhouse-gas-emissions-by-mode-of-transport/
[24] McIver, J.B., "Cessna Skyhawk II / 100 Performance Assessment," 2003. http://temporal.com.au/c172.pdf
[25] Martinez-Val, R., Perez, E., and Palacin, J.F., "Historical Evolution of Air Transport Productivity and Efficiency," *Aerospace Sciences Meetings,* Vol. 43, 2005, https://doi.org/10.2514/6.2005-121
[26] Suppes, G., and Suppes, A., "Ground Effect Vehicle," Vol. PCT/US24/35242, 2024, pp. 1–32. https://www.hs-drone.com

A. The Authors

Adam B. Suppes received his PhD in chemical and biomolecular engineering from the University of Pennsylvania, Philadelphia, PA, USA in 2022. He received his BS in chemical and biomolecular engineering from the Johns Hopkins University, Baltimore, MD, USA in 2016.
He is a researcher with HS-Drone, LLC Charlottesville, VA and researcher for his own start up Suppes Engineering Technologies, LLC. His current research includes computational fluid dynamics for ground effect vehicles and planform aircraft.

Galen Suppes (Fellow, AICHE). Dr. Suppes is the founder of HS-Drone LLC, a company specializing in digital prototypes of multimodal transportation ranging from railcars to aircraft. Dr. Suppes has over 125 refereed publications cited over 8300 times and has taught chemical engineering design for over 15 years. For 40 years his work has emphasized increased energy efficiency and sustainability including the lead of the 2006 awardee of the Presidential Green Chemistry Challenge.